JOURNAL OF GEOPHYSICAL RESEARCH, VOL. 97, NO. B4, PAGES 4349–4360, APRIL 10, 1992

Magnetic Property Zonation in a Thick Lava Flow

HARALDUR AUDUNSSON[1] AND SHAUL LEVI

College of Oceanography, Oregon State University, Corvallis

FLOYD HODGES[2]

Battelle Northwest, Richland, Washington

In this study, grain size and composition-dependent magnetic properties of titanomagnetite minerals are used as indicators of intraflow structures and magmatic evolution in an extensive and thick (30–60 m) basaltic lava flow. Similar zonation occurs in this flow at three localities separated by tens of kilometers. The magnetic properties subdivide the flow to three zones. The upper layer, representing the top 1/3 of the lava (≤ 20 m), has higher magnetic stability due to smaller and more deuterically oxidized titanomagnetite grains, approaching pure magnetite. The central layer in the underlying 2/3 of the flow (≤ 35 m) has larger, magnetically less stable, and less oxidized grains with relatively uniform magnetic properties. The basal layer, the bottom 1/10 of the flow (≤ 5 m), has near primary, least oxidized titanomagnetites ($Ulv_{68}Mag_{32}$). The upper intraflow boundary of the magnetic properties appears to coincide with the transition from entablature (above) to colonnade (below), distinguishing between regions of faster and slower cooling. Microprobe data indicate that the intraflow oxidation state (Fe^{3+}/Fe^{2+}) of the initially precipitated primary titanomagnetites increases with falling equilibrium temperature from the flow margins to a maximum near the center, the position of lowest equilibrium temperature. In contrast, Curie temperature measurements indicate that titanomagnetite oxidation increases with height in the flow. Modification of the initially symmetric equilibrium titanomagnetite compositions was caused by subsolidus high-temperature oxidation possibly due to hydrogen loss produced by dissociation of magmatic water, as well as unknown contributions of circulating air and percolating water from above. The titanomagnetites of the basal layer of the flow remain essentially unaltered.

INTRODUCTION

Background

To improve the resolution of paleomagnetic results from thermal remanent magnetization (TRM) in igneous rocks would require a more fundamental understanding of the origin and evolution of the magnetic particles, which directly reflects on remanence blocking and its stability.

In basaltic rock, the magnetic properties are due primarily to iron-titanium oxide minerals, precipitating from cooling magmas. In thick lavas a range in magmatic conditions and extended thermal histories influence the composition and oxidation trends, microscopic structures, and grain sizes of the magnetic minerals, thus controlling their magnetic behavior. Conversely, spatial variations of the magnetic properties can be useful for delineating structures and revealing aspects of magmatic and thermal evolution of volcanic bodies [*Watkins and Haggerty*, 1967].

The iron-titanium oxides are usually a late stage crystallization phase in basaltic melts at low pressure [e.g., *Hill and Roeder*, 1974]. Particle sizes of the iron-titanium oxides are related to the cooling rate of the magma, and their composition depends, in large part, on the availability of oxygen. In a quenched melt, iron-titanium oxides may comprise only a minor fraction of the crystalline rock, or be absent altogether. For slower-cooling igneous units the iron-titanium oxide grains may be larger and exhibit compositional evolution, i.e., exsolution lamellae and high-temperature oxidation [e.g., *O'Reilly*, 1984]. The composition of associations of some iron-titanium oxide phases can be used to infer the absolute temperature and oxygen fugacity at their lowest equilibrium temperature [e.g., *Buddington and Lindsley*, 1964; *Anderson and Lindsley*, 1988].

Magmatic bodies with sufficiently protracted cooling histories, such as intrusions and thick lavas, may preserve continuous records of geomagnetic secular variation. Correct interpretation of these data requires knowledge of the sequence of remanence blocking in the unit and an absolute time scale. The relative timing of blocking would be further complicated by spatial variation of the parameters that control remanence blocking within the magmatic body.

We measured profiles of different magnetic properties in a single basalt flow at several sites. The flow thickness varies from 30 to 62 m, corresponding to 10 to 50 years for the flow to have cooled everywhere to below 600°C [e.g., *Audunsson*, 1989]. Because the lava is relatively fresh, it retains much of its primary magmatic zonation. The flow has strongly layered magnetic properties, consistent with the inferred cooling history and correlated with intraflow structures as well as conditions during the initial formation of the magnetic grains.

Geological Setting

Our data are from the tholeiitic Roza Member of the middle Miocene Columbia River Basalt (CRB) Group in northwestern United States. The Roza is one of the most voluminous and extensive CRB units with estimated area and volume of 40,000 km^2 and 1500 km^3, respectively [*Swanson et al.*, 1975]. The Roza flooded across the topographically low Pasco Basin in south central Washington State from source-dikes in the southeast part of the state. The lava ponded in the Pasco Basin with thicknesses exceeding 60 m, approximately 150 km from its source.

In the Pasco Basin we sampled the Roza flow in two vertical drill cores, DC2 and DC12, 11 km apart, where the flow is 62 and 54 m thick, respectively [*Reidel and Fecht*, 1981], core recovery was nearly 100%, and the Roza appears to be a single cooling

[1]Now at Reykjavik, Iceland
[2]Now at Westinghouse, Hanford Operations, Richland, WA

Copyright 1992 by the American Geophysical Union.

Paper number 91JB01508.
0148-0227/92/91JB-01508$05.00

unit. The flow is massive throughout except near the top, which is vesicular, brecciated, and/or rubbly, and it is in sharp contact with the underlying basalt flow in DC12. A thin patch of sediment possibly occurs at the base of Roza in DC2. In DC12 and DC2 the Roza is overlain by 33- and 15-m-thick lavas, respectively. Horizontal minicores 25 mm in diameter were drilled through the 63-mm-diameter drill cores, and the centermost specimen (≤ 23 mm long) from each minicore was used for magnetic measurements. We also sampled two Roza outcrops, approximately 70 km northwest of the Pasco Basin and separated by about 30 km, where the flow is 25–35 m thick [*Mackin*, 1961; *Myers*, 1973; *Diery and McKee*, 1969]. Site locations are given in Appendix 1.

Magnetic Properties

Results From Drill Cores

The magnetic properties of the Roza flow at both drill cores (DC12 and DC2) have similar intraflow patterns. Therefore results from both sites are usually shown and discussed together. To compensate for the slightly different flow thickness in the two drill cores, the samples are assigned a normalized height from the base of the flow. Laboratory procedures are outlined in Appendix 2, and common abbreviations are listed in Table 1.

The Lowrie-Fuller test. *Lowrie and Fuller* [1971] suggested a procedure for inferring the average domain structure of magnetic grains by comparing the stabilities to alternating fields (AF) of high and low field TRM. Because basalts commonly undergo chemical changes when heated in the laboratory to even moderate temperatures and because anhysteretic remanent magnetization (ARM) usually has similar AF stability to TRM [*Levi and Merrill*, 1976], *Johnson et al.* [1975] introduced the modified Lowrie-Fuller test, where TRM is replaced by ARM.

The stabilities of ARM and saturation isothermal remanent magnetization (SIRM) to AF demagnetization are shown separately for the two drill cores in Figure 1, where the stability is measured by the median demagnetizing field (MDF, the AF required to halve the initial remanence). The stability profiles are similar for both sites: higher toward the top of the flow and uniformly lower below height 0.75 and 0.65 (corresponding to 14 and 22 m from the flow top) in DC12 and DC2, respectively. In the upper zones, low field ARM is generally more stable than SIRM, consistent with predominant single domain (SD) behavior in the framework of the Lowrie-Fuller test. In the flow interior the opposite behavior is typically observed, suggesting that multidomain (MD) grains are the more important remanence carriers. Therefore the magnetic stabilities and the Lowrie-Fuller test divide the flow to an upper layer with a higher concentration of stable SD grains, and the interior where the remanence is carried by less stable grains showing MD behavior.

TABLE 1. Abbreviations

Symbol	Name
M_s	saturation magnetization
IRM	isothermal remanent magnetization
SIRM	saturation IRM
ARM	anhysteretic remanent magnetization
NRM	natural remanent magnetization
χ_o	low field susceptibility
T_c	Curie temperature
AF	alternating fields
MDF	median demagnetizing field
SD	single domain
MD	multidomain

SIRM/M_s. SIRM/M_s is 0.5 for an assemblage of randomly oriented, noninteracting SD grains with monoaxial anisotropy [*Stoner and Wohlfarth*, 1948]. This ratio is expected to be considerably lower, ≤ 0.1, for the "softer" MD grains; however the transition is gradual [e.g., *O'Reilly*, 1984, Figure 7.10]. The results for 18 samples, for which both SIRM and M_s were measured, are listed in Table 2, and the ratio's intraflow variation is shown in Figure 2. The average SIRM/M_s is 0.20 in the top quarter of the flow (s.d.=0.03, N=9) and 0.11 below (s.d.=0.04, N=9). Although these values do not represent ideal behavior of either SD or MD grains, they suggest a shift of the predominant domain structure to relatively finer, magnetically more stable SD grains towards the top of the flow.

χ_o/M_s. χ_o/M_s is also a measure of the magnetic domain structure, and for small particles larger than SD it is expected to increase with increasing grain size [e.g., *Chikazumi*, 1964]. The χ_o/M_s depth relation is shown in Figure 2. The χ_o/M_s and SIRM/M_s depth profiles are inversely correlated, and they are similar in showing a transition at approximately the same level in the flow at height 0.75. χ_o/M_s is 5.7×10^{-6} m/A (s.d.=0.9×10^{-6} m/A, N=9) and 9.2×10^{-6} m/A (s.d.=1.6×10^{-6} m/A, N=9) above and below the transition, respectively.

The ratios SIRM/M_s and χ_o/M_s probe different aspects of domain structure. While χ_o/M_s is related to the reversible induced magnetization, SIRM/M_s depends on factors which affect the remanence. Thus although both parameters indicate similar changes of the magnetic particle sizes within Roza, it is not surprising that they differ in detailed variations.

M_s and SIRM. M_s and SIRM are proportional to the bulk magnetization. However, in contrast to SIRM, M_s is largely independent of domain structure. Figure 3*a* shows that both M_s and SIRM are higher near the top, the magnetically more stable part of the flow. In the flow interior, both SIRM and M_s generally decrease with depth. IRM acquisition experiments show that the external fields needed to impose about 90% SIRM increase with height in the drill cores in a regular manner from 30 to 150 mT (Figure 3*b*).

χ_o and ARM. χ_o and ARM are proportional to M_s. For small particles, the specific χ_o decreases with decreasing grain size and is lowest for stable SD particles; for MD grains, χ_o increases with particle size, finally becoming size independent [*Stacey and Banerjee*, 1974], and the transition is composition dependent. The specific ARM intensity for small MD magnetite particles decreases rapidly with increasing grain size [e.g., *Gillingham and Stacey*, 1971; *Bailey and Dunlop*, 1983]. Therefore χ_o and ARM are expected to have contrasting grain size dependences.

The relative constancy of χ_o and ARM intensity (Figure 4) in the lower 3/4 of the Roza flow in drill cores DC12 and DC2 suggests a uniform average domain structure. The increase in χ_o and ARM in the top zone is most easily explained by decreasing particle sizes and higher bulk M_s, consistent with observed stability and M_s profiles, respectively. The increase in ARM and corresponding decrease in χ_o near the base of the flow is compatible with either a decrease in particle size or an increase in titanium content of the titanomagnetites, which would, in effect, increase the critical particle size for the SD to MD transition.

T_c and high field M(T). T_c and M_s were determined for 18 Roza specimens, 14 from DC12 and 4 from DC2 (Table 2). Figure 5 shows the high field magnetization versus temperature (M_s-T) curves during heating. Heatings usually produced less than 25% change in the initial M_s (Table 2). The only exception, a 67% increase of the pre-heating M_s, occurs at 0.90 from the base of Roza. There are three groups of Curie temperatures: 90°–275°C, 490°–535°C, and 565°–580°C. By considering the Curie tempera-

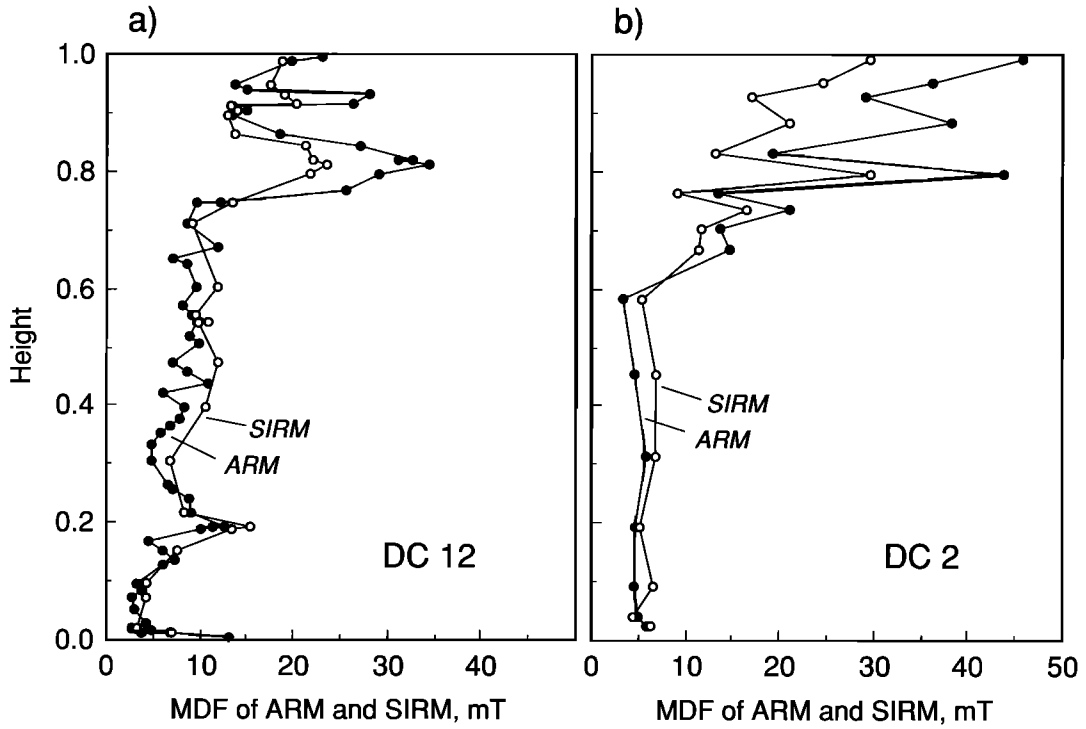

Fig. 1. Profiles of the magnetic stability (MDF) of ARM (solid circles) and SIRM (open circles) in the Roza drill cores (*a*) DC12 (54 m) and (*b*) DC2 (62 m). Sample height is given relative to normalized Roza thickness.

tures and the M_s-T curves in Figure 5, the flow may be divided to three zones with boundaries near 0.1 and 0.7–0.6 from the base of the flow. Hence both the thermomagnetic curves (mostly composition dependent) and the magnetic stability (mostly dependent on the effective particle size) detect a transition of the magnetic properties at a similar level, about 1/3 below the top of Roza.

Results From Outcrops

The Roza at both Vantage and Yakima Ridge outcrops is a single cooling unit, and only about half as thick as in the drill cores. Different intraflow structures were observed at these outcrops which are reflected in the magnetic properties.

Vantage site. At this site the flow structure is relatively simple. The lower half of the flow (~17 m) is composed of regular columns, approximately 1 m across, overlain by swirls, curved and thin columnlike pieces, up to 0.3 m wide. The flow is topped by an irregular entablature.

Magnetic property profiles for the Vantage outcrop , and the distinct colonnade to entablature transition are shown in Figure 6. The magnetic stability (MDF) of ARM, susceptibility, and Curie temperatures are generally higher in the entablature, indicating

TABLE 2. Magnetic Properties of Drill Core Samples

Specimen	Relative height	T_c, °C on heating	T_c, °C on cooling	f	M_s, A m^2/kg	SIRM, A m^2/kg	χ_o, $\times10^{-6}$ m^3/kg	SIRM/M_s	χ_o/M_s 10^{-6} m/A	MDF of ARM, mT
D1	0.952	575	575	0.87	2.4	0.55	13	0.23	5.4	36
S1	0.949	235 580	~245 550	0.85	1.9	0.39	9	0.21	4.9	14
R9	0.931	565	565	0.96	3.0	0.52	18	0.17	5.9	28
S2	0.902	390 575	420 570	1.67	1.6	0.28	9	0.18	5.9	15
D2	0.884	505	455	0.96	1.7	0.38	12	0.22	6.9	38
S3	0.864	(200) 510	~380 ~475	1.07	1.5	0.24	11	0.16	7.1	18
S4	0.845	(245) 525	440	1.15	1.8	0.33	9	0.18	4.9	27
R11	0.811	570	560	0.94	2.1	0.51	11	0.24	5.0	34
S5	0.796	565	560	0.96	2.5	0.48	12	0.19	4.9	29
S6	0.712	<350 520	350	0.90	1.4	0.12	10	0.09	7.1	9
D3	0.584	260 <515	210	0.86	1.1	0.06	11	0.05	9.6	3
R12	0.541	~285 505	335 ~420	1.15	1.1	0.17	8	0.15	7.2	10
S9	0.398	(205) 490	250 ~495	0.85	1.2	0.15	10	0.13	8.5	8
R13	0.193	(225) 525	365	0.89	1.0	0.18	9	0.18	9.4	13
S11	0.151	175 <495	195 (420)	0.87	1.1	0.12	9	0.11	8.0	6
R14	0.098	160	125	0.85	0.8	0.06	9	0.08	11.8	3
D4	0.041	275	225	0.85	1.1	0.09	11	0.08	10.3	5
S12	0.022	95	80	0.78	1.1	0.13	12	0.12	10.6	3

T_c values in parentheses indicate a minor phase. f, relative change in M_s due to heating: M_s (after)/M_s (before). Magnetic parameters are abbreviated in Table 1, and laboratory procedures are described in Appendix 2. Specimens labeled D are from DC2 and those designated by S and R are from DC12. S specimens were also analyzed on the electron microprobe (Tables 3 and 4).

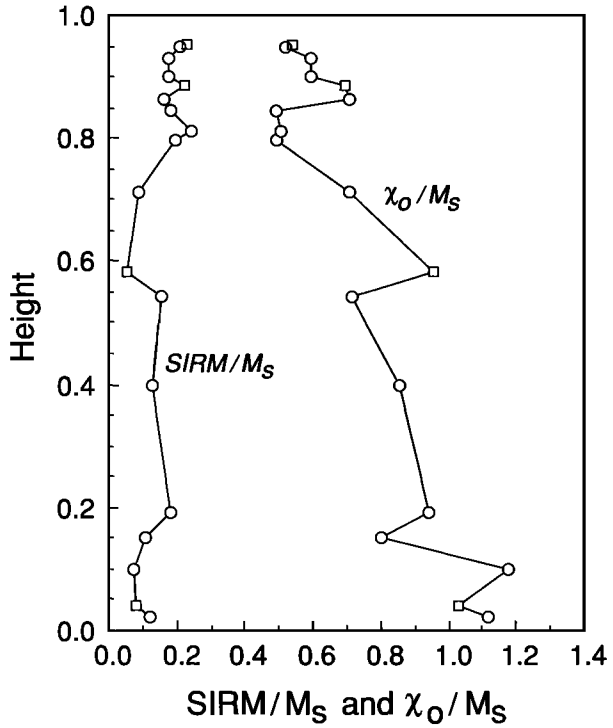

Fig. 2. Intraflow variation of the magnetic stability index SIRM/M_s (unitless) and χ_o/M_s (10^{-5} m/A) in the Roza drill cores. These data are consistent with higher concentration of smaller magnetic particles toward the top of the flow. Circles and squares represent specimens from DC12 and DC2, respectively.

smaller and more oxidized grains than in the underlying columns. Data from the lowest cluster at the base of the flow, height 0.4 m, appear distinct from the colonnades and may reflect high gradients due to the proximity to the flow's lower boundary. The intraflow pattern of the magnetic properties are consistent with the results from the drill cores.

Yakima Ridge site. At this site the Roza flow has complex structure and no simple depth variation. There are radiating, curved, and undulating columns and possible internal flow features. The Curie points have no consistent pattern, and the M_s-T curves show predominantly low T_c values with tails extending to higher temperatures. No simple depth dependence is evident for χ_o or M_s.

Opaque Grain Size, Mode, and Composition

The tholeiitic Roza flow is characterized by large plagioclase phenocrysts, and in DC12 there are no trends in the bulk composition profiles with FeO = 14.3 and TiO_2 = 3.0 wt % (E.P. Verplanck and M.R. Fisk, unpublished manuscript, 1989).

Mode of Opaque Grains and Sizes

The modal concentration of opaque minerals in four thin sections from DC2 is 4.0% (3.1–5.7%), estimated by point count with a reflected-light optical microscope. In DC12 the mode is 6.0% (4.0–8.2%), in 13 thin sections (E.P. Verplanck and M. R. Fisk, unpublished manuscript, 1989). Based in part on the magnetic properties, we conclude that differences in the abundance of opaque grains between the two sites are probably not significant, and reflect the scatter in the estimates.

The size of the largest opaque grains increases by an order of magnitude from the edges to the center of the flow, with parallel changes in grain morphology. As a measure of grain size, we use only the diameter of the largest grains, because of sampling biases introduced in measuring smaller grains [e.g., *Kellerhals et al.*, 1975]; all measurements were done in reflected light. The profile of the maximum size of the opaque grains in Roza drill cores DC12 and DC2 is shown in Figure 7*a*, and within-sample size distributions in Figure 7*b*.

In the interior of the flow, the titanomagnetite grains are predominantly equant, up to 400 μm in diameter; needle-shaped particles are rare. These large grains also have large hemoilmenite oxidation-exsolution lamellae with localized much finer lamellae, as well as small isolated ilmenite grains. The maximum grain sizes near the top and base of the flow (height ≥ 0.85 and ≤ 0.05) are comparable, about 40 μm, but the grain shapes are different. Near the top the grains are either equant or needle-shaped. The needles are 10–30 μm by 1–2 μm, typically comprising several "en echelon" groups of smaller needles; fine lamellae were observed in some grains. Near the base of the flow the titanomagnetite grains are predominantly equant and homogeneous (with respect to our optical resolution) with a size range of 5–30 μm; needle-shaped particles are rare.

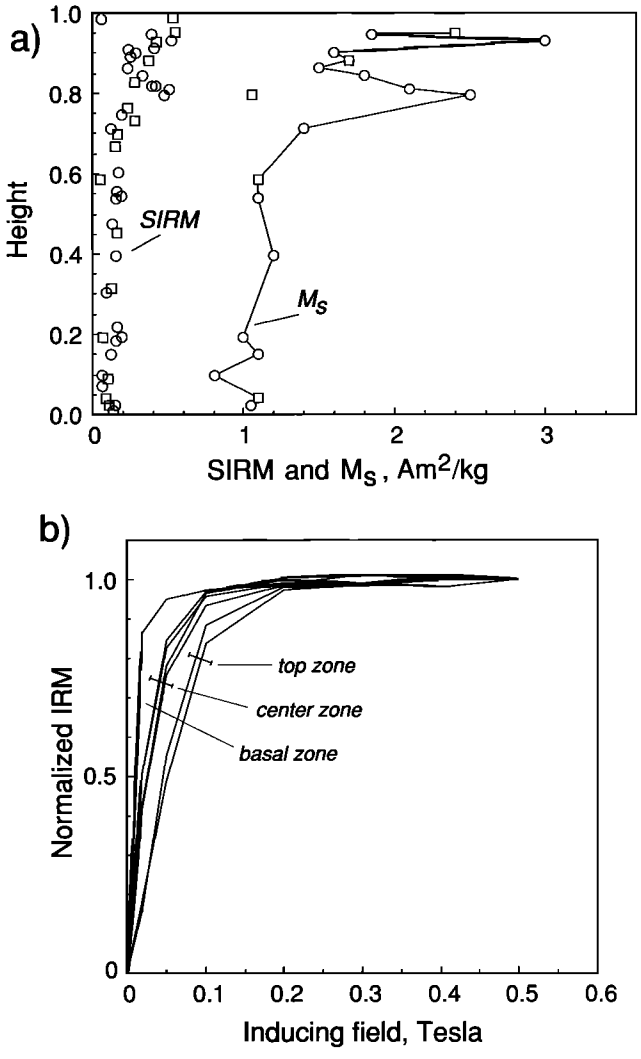

Fig. 3. (*a*) Profiles of SIRM and M_s in Roza drill cores DC2 and DC12, showing generally increasing values with height. Symbol notation is as in Figure 2. (*b*) IRM acquisition with increasing external fields for specimens from DC12. Top zone, height 0.84 and 0.92; center zone, 0.22 to 0.71; and basal zone, 0.02.

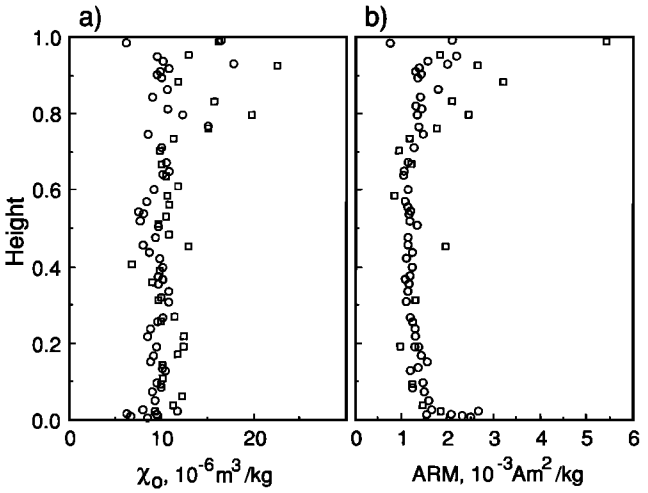

Fig. 4. Intraflow variation of (*a*) χ_o and (*b*) ARM intensity within the Roza drill cores DC2 and DC12. Symbol notation is as in Figure 2.

Chemical Analyses of Iron-Titanium Oxides

Primary (initial precipitates from the melt) iron-titanium oxides are usually solid solutions with small concentrations of minor elements such as Mg, Al, Mn, and Cr. The iron-titanium oxides were examined with an optical microscope, and chemical compositions were determined by electron microprobe (JEOL Superprobe 733) using a 15-kV accelerating voltage, a beam current of 20 nA and a 1-μm beam diameter. Because oxygen was not included in the analyses, stoichiometry was assumed for calculating the compositions of the titanomagnetite and hemoilmenite solid solutions. Summary electron microprobe analyses of the iron-titanium oxides at different levels in the Roza flow are listed in Table 3, and typical analyses are shown in Table 4.

The chemical analyses are recalculated to yield the ulvöspinel and ilmenite components of the solid solutions by allocating the minor elements to iron (denoted by X_t and Y_i for Ulv_XMag_{1-X} and Ilm_YHem_{1-Y}, respectively) [e.g., *O'Reilly*, 1984, pp. 9 and 137]. Table 3 lists the bulk composition of the titanomagnetites, hemoilmenites, and the average minor element concentration.

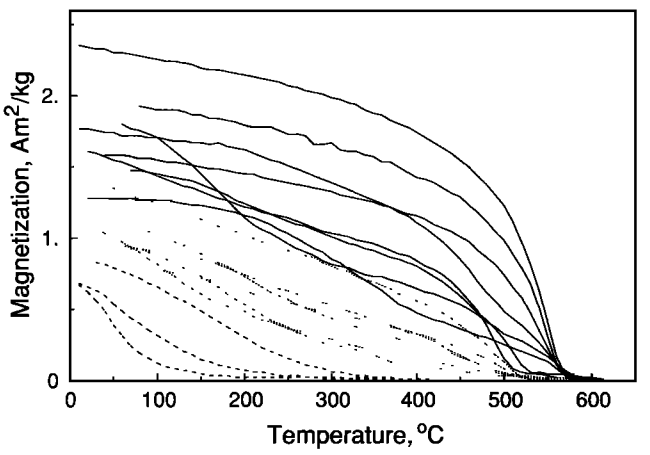

Fig. 5. High field magnetization versus temperature of 18 specimens from different intraflow levels from both drill cores, showing a general increase in T_C with height. The solid, dotted, and dashed lines are for specimens from the top, center, and basal zones of the flow, respectively (see Table 2).

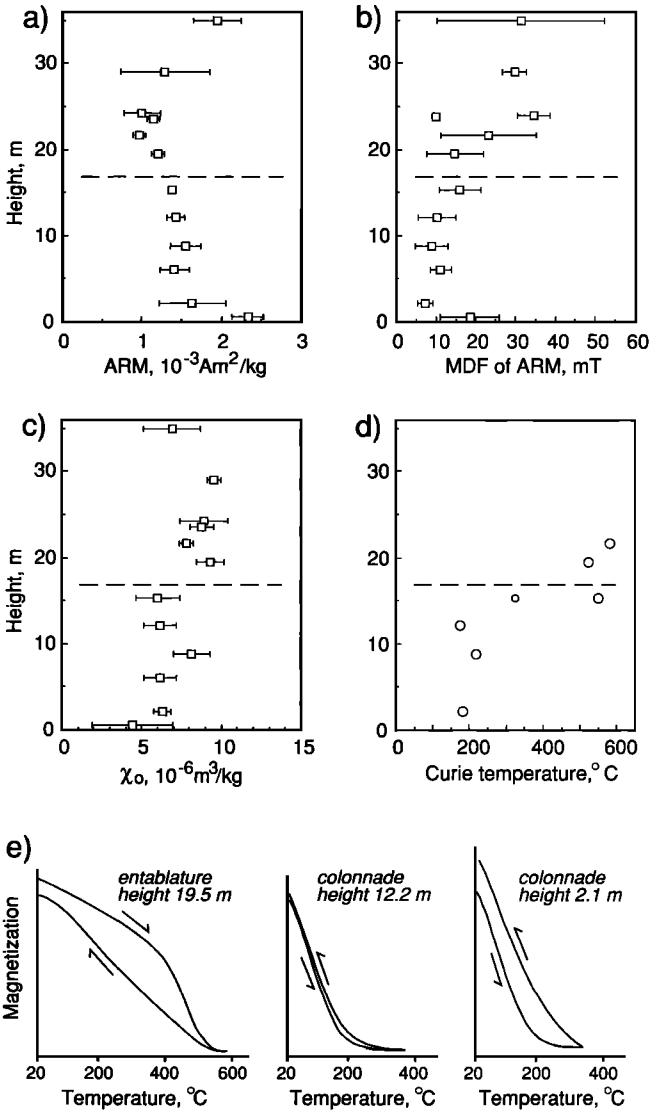

Fig. 6. Profiles of magnetic properties in the Roza outcrop at the Vantage site, which has regular intraflow structure: (*a*) magnetic intensity, (*b*) remanence stability, (*c*) low field susceptibility, (*d*) Curie temperatures, and (*e*) examples of high field magnetization versus temperature curves in the entablature and colonnade. The squares and error bars in Figures 6*a*, 6*b*, and 6*c* represent mean values and one standard deviation of clusters of two to five specimens at each level. The dashed horizontal line shows the mapped colonnade-entablature boundary.

There is no evidence for depth dependence of any of the minor elements. Ignoring the minor elements and computing X in Ulv_XMag_{1-X} solely from the ratio Ti/Fe (denoted by X_r) results in values higher by about 0.02. A scheme by *Stormer* [1983], thought to be compatible with the thermodynamics of the coexisting titanomagnetite and hemoilmenite phases [*Anderson and Lindsley*, 1988] leads to consistently higher values (denoted by X_s): $X_s - X_i \approx 0.04$ on average (Table 4).

The computed titanomagnetite and hemoilmenite compositions for the Roza flow (Figure 8) exhibit a continuous variation with depth. The ulvöspinel fraction (X_t) decreases symmetrically from a maximum value $Ulv_{68}Mag_{32}$ near the top and base to a minimum value of $Ulv_{47}Mag_{53}$ near the center of the flow. There is a parallel increase of the titanomagnetite ferric/ferrous ratio. The hemoilmenites (Y_t) are essentially uniform with depth, $Ilm_{94}Hem_6$. Similar trends in titanomagnetite evolution were

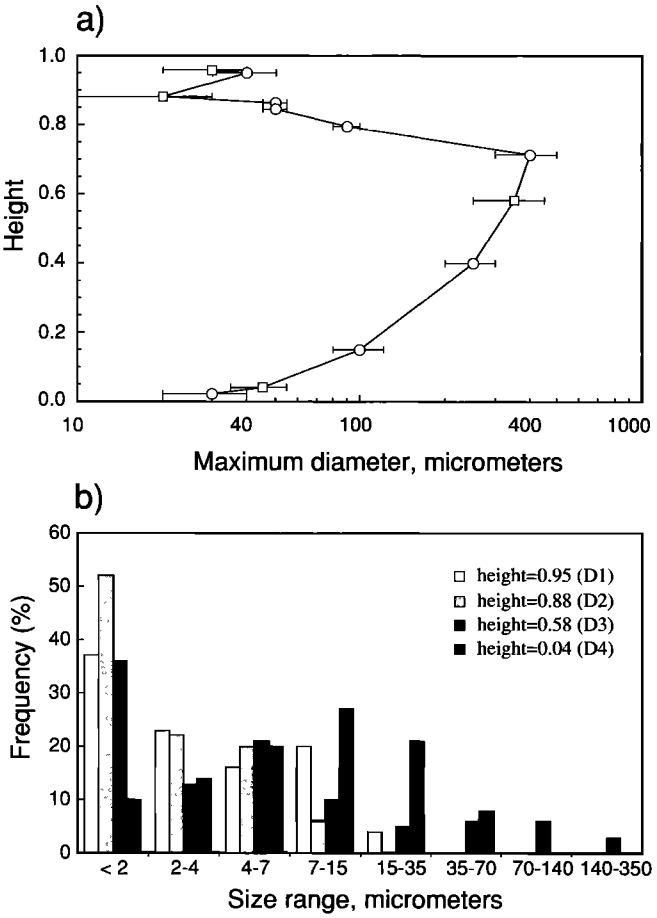

Fig. 7. Intraflow grain sizes of opaques. (*a*) Maximum size of opaque grains at different levels in the flow. Symbol notation is as in Figure 2. (*b*) Size distribution at particular levels in DC2.

observed from the optical mineralogy of some lavas from Iceland [*Watkins and Haggerty*, 1965 and 1967] and a 13 m flow from the Cretaceous Rajmahal volcanics, Bihar [*Nag and Mallik*, 1983].

Discussion

Magnetic Zonation

The profiles of the measured magnetic properties of the Roza flow are similar in the two drill cores, separated by about 11 km, indicating that the observed zonation is not a random local feature, but rather it reflects more general processes. The Roza is a single cooling unit in the two drill cores, as suggested by the visual core descriptions, vertical profiles of the magnetic properties, absence of oxidized or vesicle zones within the flow as well as the grain size distributions of different minerals.

The magnetic stability and intensity divide the flow in two primary zones and possibly a third thin basal layer: (1) The top zone, ~1/3 of the flow thickness (15–20 m), has higher magnetic stability and magnetization than below, resembling SD behavior. (2) The interior 2/3 (35–40 m) of the flow has relatively uniform magnetic properties and lower magnetic stability, more typical of larger MD grains. (3) The basal layer, the flow's bottom few meters, is characterized by the lowest measured T_c values, somewhat higher ARM intensity and higher stability.

Magnetic stability and relative particle size. The higher magnetic stability in the upper zone is mostly due to a larger fraction of smaller magnetic particles than deeper in the flow. However, it is often difficult to assess the influence of competing variables on the stability such as particle size, shape and composition. For similar domain structure in particles larger than SD, the parameter SIRM /M_s is expected to be lower in magnetite grains than for titanomagnetites [e.g., *Dunlop*, 1983]. Furthermore, in titanomagnetites the critical SD size increases with titanium content [e.g., *Chikazumi*, 1964, p. 240]. Therefore the small increase in magnetic stability near the base of the flow may result from titanium enrichment in the titanomagnetites, rather than being solely a reflection of smaller particle sizes. This is supported by lower T_c values and microprobe analyses.

The rather poor correlation between the optically observed maximum grain sizes (Figure 7) and the depth profiles of the magnetic stability (Figures 1 and 2) is not surprising, because the stable remanence in titanomagnetite minerals resides in grains smaller than a few tens of microns, and frequently in the submicron size range, with little or no relationship to the maximum particle sizes. This observation was noted in earlier studies [e.g., *Graham*, 1953; *Wilson et al.*, 1968].

Intraflow structures. In drill cores it is not possible to deduce the macroscopic structural flow features that are readily mapped in outcrop; however, visual observations of the cores show that vertical fractures predominate from the base to heights 0.73 and 0.78 in DC12 and DC2, respectively. Above these levels the fractures are mostly horizontal or irregular. This change in the fracture pattern may indicate the boundary between the colonnade

TABLE 3*a*. Bulk Composition of Titanomagnetites and Hemoilmenites

Specimen	Relative Height	Titanomagnetites						Hemoilmenites				
		n	*X*	s.d.	min/max	W_X	s.d.	*n*	*Y*	s.d.	W_Y	s.d.
S1	0.949	6	0.69	0.03	0.66/0.75	4.9	0.7	3	0.93	0.01	2.9	0.1
S2	0.902	8	0.66	0.05	0.57/0.73	5.1	0.4	5	0.94	0.01	3.2	0.1
S3	0.864	5	0.63	0.07	0.55/0.71	5.0	0.8	5	0.93	0.02	3.1	0.4
S4	0.845	4	0.59	0.03	0.56/0.62	5.0	0.1	6	0.92	0.04	3.1	0.2
S5	0.796	3	0.64	0.07	0.58/0.71	4.7	0.3	4	0.94	0.01	4.0	0.7
S6	0.712	5	0.59	0.02	0.57/0.61	5.4	0.3	6	0.96	0.01	3.4	0.2
S7	0.649	9	0.56	0.04	0.51/0.61	3.4	0.5	7	0.94	0.01	2.3	0.4
S8	0.508	6	0.60	0.03	0.57/0.66	4.6	0.5	8	0.96	0.01	3.1	0.3
S9	0.398	6	0.46	0.07	0.36/0.52	4.1	0.4	8	0.94	0.01	3.5	0.5
S10	0.266	7	0.52	0.04	0.45/0.56	4.0	0.2	9	0.94	0.01	2.5	0.5
S11	0.151	5	0.58	0.02	0.55/0.60	4.9	0.4	6	0.95	0.01	3.3	0.4
S12	0.022	18	0.67	0.02	0.59/0.70	4.0	0.5	2	0.94	0.01	1.7	0.2

n, number of analyses; *X* and *Y* in Ulv_XMag_{1-X} and Ilm_YHem_{1-Y} are computed as $(Fe,Al,Mg,Mn,Cr)_{3-X}Ti_XO_4$ and $(Fe,Al,Mg,Mn,Cr)_{2-Y}Ti_YO_3$, denoted as X_t and Y_t in the text, respectively; s.d., standard deviation; min/max, minimum/maximum value of *X*, based on individual analyses; *W*, minor elements as percent of total anions.

TABLE 3*b*. Minor Elements

	Al(3+)	Mg(2+)	Mn(2+)	Cr(3+)	Total
Titanomagnetites	0.079±0.011	0.038±0.008	0.018±0.005	0.004±0.001	0.138±0.018
Hemoilmenites	0.003±0.001	0.045±0.011	0.013±0.002	<0.001	0.060±0.012

Average microprobe analyses with associated standard deviations of the 12 specimens in Table 3*a*. Data represent number of cations per formula unit. There are 3 and 2 cations in titanomagnetites and hemoilmenites, respectively.

(below) and entablature (above), and it correlates precisely with the transition in the magnetic properties in DC12, but is slightly lower in DC2 (e.g., Figures 1 and 2). The change from smaller, magnetically more stable, particles in the rapidly cooled top zone to larger, less stable, particles lower in the flow is consistent with an entablature/colonnade transition [*Long and Wood*, 1986; *DeGraff et al.*, 1989]. The grain size is maximum near 0.7 from the base (Figure 7), and the glass content (E.P. Verplanck and M.R. Fisk, unpublished manuscript, 1989) is minimum near the level 0.7–0.8, similar to the results of *Long et al.* [1980], who showed that the entablature/colonnade transition is associated with a change in the glass abundance. The correlation of magnetic properties and flow morphology is supported by the results from the outcrop near Vantage, where the magnetic stability, susceptibility and Curie temperatures are higher in the entablature than in the colonnade (Figure 6). Moreover, in both the Vantage outcrop and drill core DC12 there is a distinct thin basal zone, of the order of a few meters or less.

The magnetic properties do not always show simple intraflow zonation. The outcrop at Yakima Ridge (Appendix 1) has a highly complex flow morphology with relatively poorly developed colonnade and no evident depth dependence of the magnetic properties. Intraflow complexities of the magnetic property profiles were observed in previous studies [e.g., *Petersen*, 1976; *Ade-Hall et al.*, 1968*a*,*b*; *Herzog et al.*, 1988], and the oxidation pattern may appear variable between lavas [e.g., *Watkins and Haggerty*, 1965 and 1967; *Wilson et al.*, 1968; *Nag*, 1985; *Herzog et al.*, 1988]. In relatively thin lava flows, high-temperature chemical evolution may be limited by the rapid cooling, and the variation in magnetic properties may be as large laterally as vertically [e.g., *Ade-Hall et al.*, 1968*a*,*b*], possibly due to the relatively larger influences of processes near the boundaries. In addition, low-temperature alteration may subsequently change the initial within-flow zonation of the iron-titanium oxides and the magnetic properties.

Observed T_c and high field M(T). The two primary zones identified in the Roza drill cores from the intraflow magnetic stability are essentially repeated in the depth profile of the Curie points and patterns of the M_s-T curves. In addition, these data define a thin basal zone in the lowest few meters of the flow (Figures 5 and 9).

In the basal zone, the T_c values are between 90°–275°C, and the iron-titanium oxides appear to represent primary compositions, typical of rapidly cooled, unaltered tholeiitic basalts [*Petersen*, 1976]. This composition probably reflects the oxygen fugacity and temperature conditions early in the lava's thermal history, preserved in the rapidly cooled flow base. The absence of exsolution lamellae in the titanomagnetites supports this conclusion.

The titanomagnetites from the central zone are richer in the magnetite component and have Curie temperatures approaching 500°C; however, most samples from this zone have secondary magnetic phases with T_c from 175° to 285°C (Table 2). From the intraflow trends of T_c and M_s, it appears that the titanomagnetites in the lower half of the flow evolved from a primary composition similar to that near the base. M_s-T curves show that the magnetization intensity of the higher and lower T_c phases are comparable. Because $M_s \propto T_c$ in titanomagnetite, the volume fraction of the lower T_c phase is proportionately higher. In addition, the higher T_c phases seem to consist of smaller grains than the lower T_c phases, as is suggested by their higher remanence stability (Figure 10), and smaller particles are expected to be more pervasively affected by subsolidus oxidation. Therefore it is concluded that phases with the higher T_c are predominantly products of deuteric oxidation of the primary titanomagnetites, rather than low-temperature titanomaghemitization; this is further discussed below.

The flow's top zone is more complex. In some specimens, T_c ranges between 200° and 580°C. The titanomagnetite in the upper layer is more oxidized than lower in the flow, as indicated by higher M_s and T_c values and the relatively greater intensity of the higher T_c phases (Figure 5). The most oxidized zones are at heights 0.95 to 0.90 and 0.80, with apparently nearly pure magnetite ($T_c \sim 580$°C), probably due to subsolidus oxidation. Similar compositional zonation has been observed in some Icelandic lavas [*Schönharting*, 1969].

Titanomaghemite is produced during low-temperature oxidation of titanomagnetite. In the Roza flow there is no optical evidence, such as oxidized rims, to suggest that maghemitization had occurred. However, maghemitization of smaller grains near or below the optical resolution of the microscope cannot be ruled out. Titanomaghemite is usually unstable at temperatures of a few hundred degrees Celsius [e.g., *Verhoogen*, 1962; *O'Reilly*, 1984, p. 162], and the transformation is often accompanied by substantial changes in M_s and T_c. Hence, M_s-T experiments can be diagnostic for the presence and characterization of titanomaghemites [*Ozima and Ozima*, 1971]. For all but one specimen, changes in the room temperature M_s after heating were less than 22% (Table 2), further suggesting that the Roza titanomagnetites were not significantly affected by low-temperature oxidation. Two or three specimens from the upper zone had at least two T_c, and the intensity of the higher T_c phase ($\geq$ 500°C) decreased after heating, probably due to reduction or mixing of the deuterically oxidized and exsolved titanomagnetite. M_s increases with height in the flow (Figure 3), which is more likely caused by increased deuteric oxidation than maghemitization [e.g., *O'Reilly*, 1984, p. 158], which, we believe, occurs only to a limited extent in Roza.

Observed Versus Predicted Curie Temperatures

Curie points and microprobe analyses of Roza show an evolution of the primary titanomagnetites from the initially precipitated composition, $Ulv_{68}Mag_{32}$, to much more oxidized iron rich species of almost pure magnetite. (The latter observation is based only on Curie point measurements.)

T_c values of the titanomagnetite solid solution vary approximately linearly in proportion to the concentration of the end members [e.g., *O'Reilly*, 1984, p. 136], obeying the empirical

TABLE 4*a*. Typical Microprobe Analyses of Titanomagnetites

Section	Relative	Analyzed Oxides, wt %								Number of Cations per Formula Unit (3 Total)									
-Analysis	Height	FeO	Fe_2O_3	TiO_2	MnO	Al_2O_3	MgO	Cr_2O_3	Sum	Fe^{2+}	Fe^{3+}	Ti^{4+}	Mn^{2+}	Al^{3+}	Mg^{2+}	Cr^{3+}	X_s	X_r	X_t
S1-3	0.949	50.04	20.55	22.97	0.64	1.74	0.63	0.05	96.61	1.606	0.594	0.663	0.021	0.079	0.036	0.002	0.710	0.695	0.663
S2-13	0.902	50.78	21.96	23.14	0.65	1.78	0.76	0.09	99.16	1.588	0.618	0.651	0.021	0.078	0.042	0.003	0.696	0.683	0.651
S3-1	0.864	49.57	25.70	21.46	0.51	1.70	0.74	0.10	99.78	1.544	0.720	0.601	0.016	0.075	0.041	0.003	0.641	0.629	0.601
S4-8	0.845	49.51	25.23	21.33	0.54	2.08	0.67	0.14	99.49	1.544	0.708	0.598	0.017	0.091	0.037	0.004	0.649	0.630	0.598
S5-4	0.796	48.97	27.06	20.55	0.30	1.97	0.73	0.10	99.67	1.526	0.759	0.576	0.009	0.087	0.041	0.003	0.622	0.604	0.576
S6-5	0.712	50.47	25.64	21.75	0.43	2.29	0.80	0.14	101.52	1.540	0.704	0.597	0.013	0.098	0.044	0.004	0.652	0.630	0.597
S7-12	0.649	48.81	28.47	20.01	0.40	1.48	0.39	0.14	99.70	1.529	0.803	0.564	0.013	0.065	0.022	0.004	0.599	0.584	0.564
S8-15	0.508	50.21	24.83	21.90	0.52	2.02	0.75	0.18	100.41	1.551	0.690	0.608	0.016	0.088	0.041	0.005	0.659	0.640	0.608
S9-9	0.398	46.62	33.24	17.76	0.42	1.51	0.54	0.10	100.19	1.455	0.934	0.498	0.013	0.066	0.030	0.003	0.527	0.518	0.498
S10-3	0.266	47.74	31.16	18.90	0.51	1.44	0.46	0.11	100.32	1.488	0.874	0.530	0.016	0.063	0.026	0.003	0.559	0.550	0.530
S11-2	0.151	49.51	26.83	20.80	0.38	2.04	0.62	0.16	100.34	1.533	0.748	0.579	0.012	0.089	0.034	0.005	0.629	0.608	0.579
S12-10	0.022	50.63	20.63	23.36	0.47	1.41	0.68	0.05	97.23	1.617	0.593	0.671	0.015	0.063	0.039	0.002	0.708	0.699	0.671

Weight percent of Fe_2O_3 is computed by assuming stoichiometry. The different schemes for computing Ulv_XMag_{1-X} and Ilm_YHem_{1-Y} are: X_s and Y_s is the scheme by *Stormer* [1983]; X_r and Y_r use only the relative proportions of Fe and Ti, i.e., ignoring the minor elements; X_t and Y_t allocate the minor elements (Mn, Al, Mg, and Cr) to Fe.

TABLE 4*b*. Analyses of Hemoilmenites

Section	Relative	Analyzed Oxides, wt %								Number of Cations per Formula Unit (2 Total)									
-Analysis	Height	FeO	Fe_2O_3	TiO_2	MnO	Al_2O_3	MgO	Cr_2O_3	Sum	Fe^{2+}	Fe^{3+}	Ti^{4+}	Mn^{2+}	Al^{3+}	Mg^{2+}	Cr^{3+}	Y_s	Y_r	Y_t
S1-5	0.949	40.03	8.32	47.37	0.72	0.10	1.03	0.03	97.60	0.862	0.161	0.918	0.016	0.003	0.040	0.001	0.917	0.945	0.918
S2-14	0.902	41.70	7.24	49.57	0.59	0.12	1.28	0.00	100.49	0.870	0.136	0.930	0.012	0.004	0.048	0.000	0.930	0.961	0.930
S3-4	0.864	41.33	7.38	49.26	0.64	0.10	1.30	0.02	100.03	0.867	0.139	0.929	0.014	0.003	0.049	0.000	0.928	0.960	0.929
S4-10	0.845	41.76	5.79	49.68	0.61	0.14	1.29	0.06	99.33	0.881	0.110	0.942	0.013	0.004	0.049	0.001	0.943	0.975	0.942
S5-6	0.796	40.85	5.90	50.73	1.01	0.02	2.10	0.06	100.67	0.846	0.110	0.944	0.021	0.001	0.077	0.001	0.942	0.994	0.944
S6-3	0.712	42.56	4.22	51.05	0.56	0.07	1.56	0.01	100.03	0.889	0.079	0.959	0.012	0.002	0.058	0.000	0.959	0.995	0.959
S7-15	0.649	43.29	5.56	50.46	0.48	0.05	0.90	0.01	100.75	0.903	0.104	0.947	0.010	0.001	0.033	0.000	0.947	0.969	0.947
S8-12	0.508	42.47	4.68	50.68	0.67	0.05	1.36	0.00	99.91	0.890	0.088	0.955	0.014	0.001	0.051	0.000	0.954	0.988	0.955
S9-11	0.398	43.07	5.73	50.96	0.57	0.08	1.22	0.02	101.65	0.889	0.106	0.945	0.012	0.002	0.045	0.000	0.945	0.974	0.945
S10-4	0.266	41.64	7.09	48.73	0.62	0.05	0.87	0.00	99.00	0.885	0.136	0.931	0.013	0.001	0.033	0.000	0.931	0.954	0.931
S11-3	0.151	43.22	4.74	50.99	0.52	0.06	1.18	0.06	100.77	0.899	0.089	0.954	0.011	0.002	0.044	0.001	0.954	0.982	0.954
S12-1	0.022	42.61	7.58	48.88	0.57	0.10	0.43	0.00	100.17	0.898	0.144	0.927	0.012	0.003	0.016	0.000	0.927	0.941	0.927

See Table 4*a* footnotes.

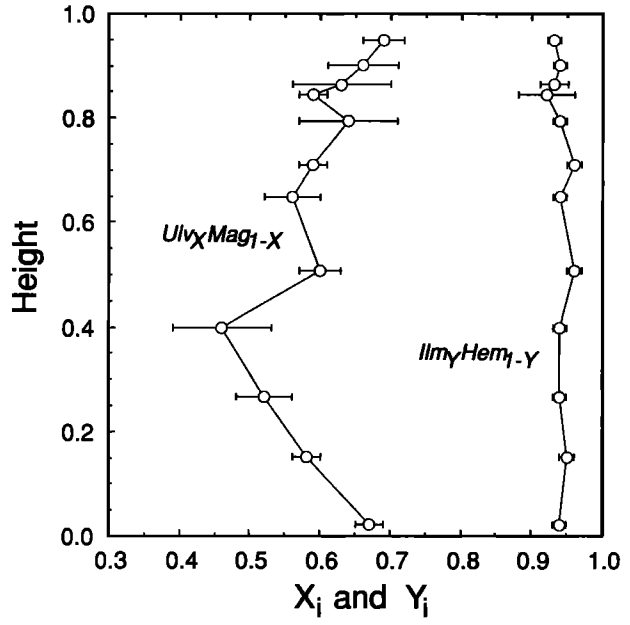

Fig. 8. Compositions in the Roza flow, inferred from the microprobe analyses of titanomagnetites, Ulv_XMag_{1-X}, and of hemoilmenites, Ilm_YHem_{1-Y}, showing higher titanomagnetite oxidation toward the flow's center. The error bars represent one standard deviation of several analyses for each sample (Table 3*a*).

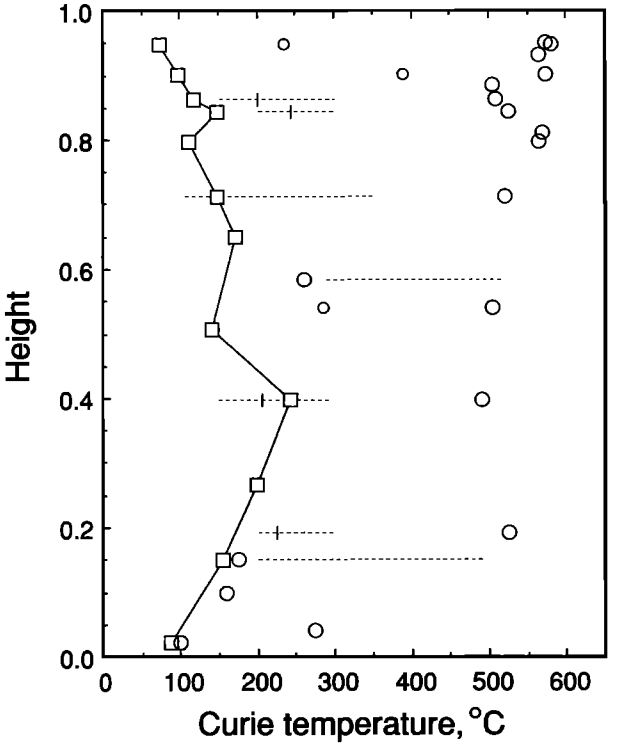

Fig. 9. Variation of measured and predicted Curie temperatures within the Roza flow. Larger circles represent the predominant higher temperature T_c; smaller circles denote the lower T_c when two phases were present; dashed lines indicate the range of T_c when a continuous distribution was observed, and a short vertical bar denotes the preferred value, possibly of a distinct phase. The predicted T_c values, calculated from bulk compositions of the titanomagnetites, are represented as connected squares (Table 3*a*).

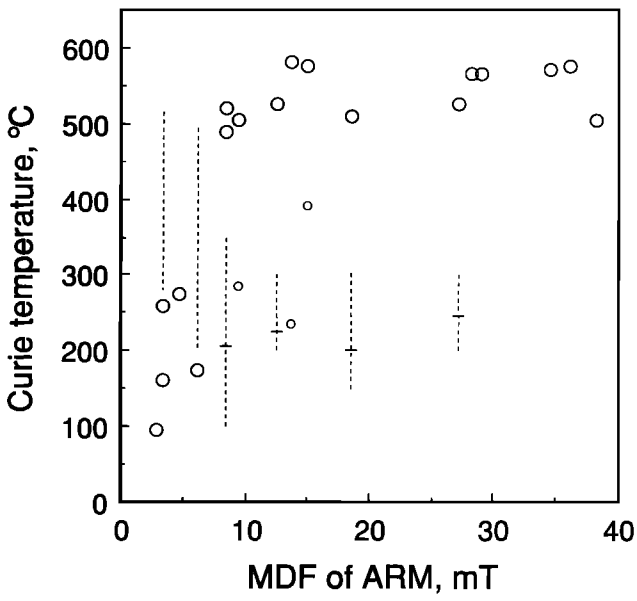

Fig. 10. Magnetic stability versus Curie temperatures in the Roza flow. The symbols are as in Figure 9.

relation $T_c = 580 - 733 \times X$ (°C), where X is the ulvöspinel fraction in Ulv_XMag_{1-X}. The abundance of minor elements (Table 3*b*) predicts a decrease in T_c by approximately 45°C [*Richards et al.*, 1973]. Predicted T_c values, neglecting the minor elements, are shown in Figure 9. However, the minor elements were considered in calculating X.

In the basal zone the measured Curie temperatures are low ($T_c \leq 275$°C) in agreement with the compositions derived from microprobe analyses (Figure 9). In the lower two-thirds of the flow the Curie temperatures vary between 95° and 520°C, but only the lower values are compatible with the microprobe compositions. In the upper one-fourth of the flow the measured T_c are considerably higher than those deduced from the microprobe compositions.

The discrepancy between the measured and predicted Curie temperatures is probably caused by the presence of more oxidized submicroscopic titanomagnetite grains. In the upper half of the flow, submicron exsolution lamellae in the titanomagnetites were observed. Therefore it is likely that the diameter of the microprobe beam was too large to resolve these and still finer exsolution lamellae, as well as smaller and more oxidized particles. Hence microprobe analyses of some of the coarser opaque grains may represent an average composition of two phases, and the calculations, indicating primary compositions, might be misleading.

Evolution of High-Temperature Oxidation

According to *Buddington and Lindsley* [1964] (see also *Anderson and Lindsley* [1988]) the equilibrium compositions of coexisting phases of iron-titanium oxides reflect the temperature and oxygen fugacity at which these minerals last equilibrated. Using the scheme by *Stormer* [1983] to compute the proportion of solid solution end-members (X_s and Y_s in Table 4), the variations in composition of the titanomagnetites and hemoilmenites indicate decreasing equilibrium temperatures from approximately 1060°C at the edges to 760°C near the center of the flow, with a corresponding decrease in oxygen fugacity from 10^{-11} to 10^{-17} bars, respectively. All the titanomagnetite-hemoilmenite pairs

used in Figure 11 satisfy the required equilibrium partitioning for Mg and Mn between these phases [*Bacon and Hirschmann*, 1988]. The compositions of the iron-titanium oxides closely follow the equilibrium temperatures and oxygen fugacities of the fayalite-magnetite-quartz buffer (Figure 11), which is common in basalt lavas [e.g., *Haggerty*, 1976]. Therefore these data show no variation in the relative oxidation state of the primary iron-titanium oxides (i.e., the system is buffered with respect to oxygen).

The microprobe-measured bulk compositions of the titanomagnetites have symmetric intraflow distribution with highest ferric content (Fe^{3+}/Fe) near the center and lowest at the margins of the flow. While the microprobe analyses represent iron-titanium oxide compositions near the lowest thermal equilibrium temperature, the increase in measured T_c and M_s with height in the Roza flow indicates that further titanomagnetite oxidation occurred at lower temperatures. Reflected light microscopy and nearly reversible M_s-T curves suggest that there was no significant low-temperature oxidation of Roza titanomagnetites. Hence we argue that the subthermal equilibrium oxidation, which increases with height in the flow, is of deuteric origin.

The gradient of the subthermal-equilibrium oxidation within the flow may result from high-temperature dissociation of water in the magma, producing hydrogen and oxygen. The hydrogen escapes the flow more readily and the oxygen concentration increases with height in the flow due to either cumulative filtration of oxygen from greater depths or due to the increased hydrogen loss toward the flow's upper surface, thereby producing a gradient in the oxygen content [e.g., *Butler and Burbank*, 1929; *Osborn*, 1959; *Sato and Wright*, 1966]. In addition, percolating water from above and circulation of atmospheric oxygen may also add to the more extensive flow-top oxidation.

The compositional differences between the microprobe analyses and measured T_c data are due to the presence of at least two families of titanomagnetite particles. Of these, the submicroscopic particles are not resolved and not examined by the microprobe, and, by virtue of their small size, they are more pervasively oxidized at subsolidus temperatures. The existence of these submicroscopic titanomagnetite particles is indicated by higher remanence-stabilities and magnetization intensities associated with higher Curie points.

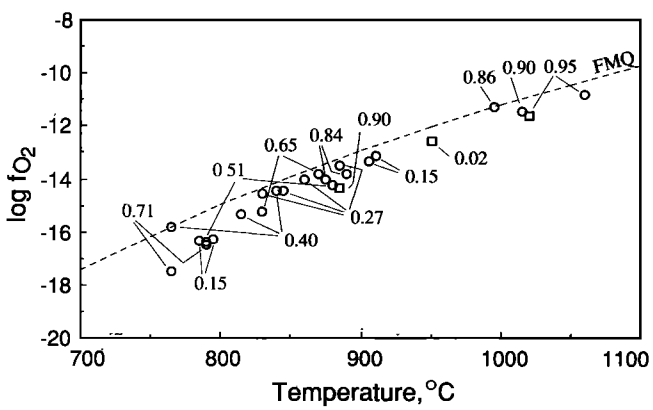

Fig. 11. Predicted oxygen fugacity and temperature at which the iron-titanium oxides last equilibrated, using microprobe compositions (X_s and Y_s) of separate grains (1 to 4 in each sample). Circles (squares) denote values from composite (isolated) grains. Numbers represent the relative intraflow heights of the samples. FMQ, the fayalite-magnetite-quartz buffer ($\log_{10} fO_2 = -25738/T(°K) + 9.00$, *Wones and Gilbert* [1969].

Conclusions

The sensitivity of some magnetic properties to changes in size and composition of the magnetic grains has been used to delineate intraflow structures and magmatic evolution in the thick basaltic Roza flow. The magnetic stability, including the median demagnetizing field of ARM and SIRM, as well as SIRM/M_s, and χ_o/M_s (see Table 1 for abbreviations), vary systematically with height in the flow in the drill core sections. These properties subdivide the lava in two and, possibly, three zones. The same subdivisions of Roza are observed in two drill cores separated by 11 km, where the flow is about 54 and 62 m thick.

In the drill cores, the top zone comprises up to 1/3 of the flow thickness (15–20 m), with higher magnetic stability due to smaller magnetic particles, higher saturation magnetization (M_s), and more oxidized titanomagnetites, evident from the higher Curie points (T_c) (up to 580°C) than deeper in the flow. In the lower 2/3 of the flow (thickness of 25–35 m) the magnetic properties are nearly uniform with lower remanence stability due to larger MD grains and lower but variable T_c values ($175° \le T_c \le 520°C$). The basal zone consists of about 1/10 of the flow (~5 m) and is delimited by lower T_c values ($\le 275°C$) of the primary titanomagnetites, somewhat higher magnetic stability and ARM intensity, as well as lower χ_o. In the drill cores the intraflow boundary between the upper layer and the bulk of the flow coincides with the transition from predominantly vertical and more regular joints and fractures below to a more chaotic pattern above. A similar contrast in the magnetic properties was observed in a 35-m-thick Roza outcrop at the colonnade/entablature transition. Thus, the relationship of magnetic stability with flow structure might provide a method for identifying and distinguishing these zones where outcrop mapping is not possible.

Our results show that the magnetic properties in the Roza flow are affected by particle size variations as well as by compositional changes. Although the maximum size of the magnetic grains is approximately symmetrical about the center of the flow, the magnetic properties are not, showing that factors other than the initial crystallization determine the effective size of the magnetic particles.

As the titanomagnetites precipitated from the melt, their ferric ion concentration increased with falling equilibrium temperature and reached maximum near the flow's center, the position of lowest temperature equilibrium. Subsequent (subthermal equilibrium) deuteric oxidation increased with height, compatible with the upward increase of oxygen concentration due to water dissociation [e.g., *Butler and Burbank*, 1929; *Osborn*, 1959] and contributions from percolating water and air circulation from above during cooling. This produced the measured intraflow T_c and M_s patterns and the shapes of M_s-T curves of near continuous evolution of the titanomagnetites from a primary composition, $Ulv_{68}Mag_{32}$, near the base of the flow, increasing deuteric oxidation of the primary phases in the bulk of the flow, to almost pure magnetite in the upper layer. The base of the flow remains essentially unaltered, retaining its primary composition.

In thick lavas, analysis of the spatial distribution of the magnetic properties can be useful for identifying structures and might assist in constraining the cooling history and magmatic evolution. Furthermore, because the magnetic stability and blocking temperatures of the remanence vary significantly within units, these differences must be taken into account when interpreting paleomagnetic records from such bodies.

APPENDIX 1: LOCATION OF SITES

Drill core DC2, Pasco Basin at the Hanford Reservation. (46°34'N, 119°31'W). Roza flow is at depth 349.2 to 410.8 m below surface, which is at 174.5 m above sea level (asl).

Drill core DC12, Pasco Basin at the Hanford Reservation. (46°28'N, 119°33'W). Roza flow is at depth 409.0 to 463.3 m below surface, which is at 157.4 m asl.

Yakima Ridge outcrop (RZ20). (46°49'N, 120°21'W). About 500-m-long roadcut along Interstate 82, northbound lane, 2 km north of Squaw Creek. Flow's base is 592 m asl.

Vantage outcrop (RZ30). (46°54'N, 119°57'W). Two hills, 20-30 m high and about 300 m apart, just east of Highway 243, 5 km south of the Interstate 90 bridge (east end) crossing the Columbia river . The outcrop is east of Wanapum Dam. Base of outcrop is 244 m asl. Lower boundary of Roza is not exposed.

Subsite RZ40, Vantage. (47°2'N, 119°58'W). An approximately 35 m long roadcut in the south wall of the north alcove of Frenchman Coulee near a spiracle in Roza (Figure 5*b* of *Mackin* [1961]). Flow's base is 342 m asl. This outcrop exposes the base of Roza in contact and directly overlying a Frenchman Springs unit.

APPENDIX 2: LABORATORY PROCEDURES

ARM was produced in a constant field of 0.05 millitesla (mT) parallel to an alternating field (400 Hz), decaying smoothly to zero from a peak value of 100 mT. IRM was imposed by exposing specimens to a constant field, typically for 2 min, and a field of 0.5 T was usually required to achieve SIRM. AF demagnetization was performed with a single axis alternating fields demagnetizer, increasing the peak AF in steps of 2.5–20 mT to the maximum peak AF of 100 mT. All remanence measurements were made with a spinner magnetometer. ARM and IRM acquisitions, χ_o, and AF demagnetizations were induced and measured at room temperature.

T_c measurements were done on a Curie balance using steady fields of 0.15 T (4 of 23 specimens were run at 0.5 T). During heating the specimens were engulfed in helium gas to minimize chemical alterations. Lewis coils [*Lewis*, 1971] were used to reverse the field gradient at regular intervals to monitor weight loss on heating. Specimens weighing 7–24 mg were usually heated at 22° or 52°C/min, and the thermal lag was quantified by repeat measurements of standards at different heating rates. For five samples, T_c was determined for two specimens from each, with indistinguishable results. The T_c values were determined from the heating curves, following *Grommé et al.* [1969].

For each specimen used for T_c determination, M_s was first measured at room temperature. M_s is the magnetization in zero field, obtained by linear extrapolation of the high field magnetization curve from 1.5 T to correct for paramagnetic contributions at higher fields.

Acknowledgments. Philip Long was responsible for permission to sample the Pasco Basin drill cores; Bob Bentley showed us outcrops of the Roza flow. Dennis Schultz provided invaluable assistance both in the field and in the laboratory. We thank Robert Lewis formerly of Chevron Research Laboratories, Richmond, CA for use of his Curie balance. Additional Curie point determinations by Jean-Sebastien Salis and Francoise Calza were made at the University of Rennes, France. Anita Grunder, Peter Shive, Ken Hoffman, and Stephen Haggerty provided helpful reviews. This work was supported by grants from NORCUS and the National Science Foundation.

REFERENCES

Ade-Hall, J. M., M. A. Khan, P. Dagley, and R. L. Wilson, A detailed opaque petrological and magnetic investigation of a single Tertiary lava flow from Skye, Scotland, I, Iron-titanium oxide petrology, *Geophys. J. R. Astron Soc.*, *16*, 375–388, 1968*a*..

Ade-Hall, J. M., M. A. Khan, P. Dagley, and R. L. Wilson, A detailed opaque petrological and magnetic investigation of a single Tertiary lava flow from Skye, Scotland, II, Spatial variations of magnetic properties and selected relationships between magnetic and opaque petrological properties, *Geophys. J. R. Astron. Soc.*, *16*, 389–399, 1968*b*.

Anderson, D. J., and D. H. Lindsley, Internally consistent solution models for Fe-Mg-Mn-Ti oxides: Fe-Ti oxides, *Am. Mineral.*, *73*, 714–726, 1988.

Audunsson, H., Paleomagnetism, magnetic properties and thermal history of a thick transitional polarity lava, Ph.D. thesis, 265 pp., Oreg. State Univ., Corvallis, 1989.

Bacon, C. R., and M. M. Hirschmann, Mg/Mn partitioning as a test for equilibrium between coexisting Fe-Ti oxides, *Am. Mineral.*, *73*, 57–61, 1988.

Bailey, M. E., and D. J. Dunlop, Alternating field characteristics of pseudo-single-domain (2-14 μm) and multidomain magnetite, *Earth Planet. Sci. Lett.*, *63*, 335–352, 1983.

Buddington, A. F., and D. H. Lindsley, Iron-titanium oxide minerals and synthetic equivalents, *J. Petrol.*, *5*, 310–357, 1964.

Butler, B. S., and W. S. Burbank, The copper deposits of Michigan, *U.S. Geol. Surv., Prof. Pap.*, *144*, 1929.

Chikazumi, S., *Physics of Magnetism*, 554 pp., J. Wiley and Sons, New York, 1964.

Diery, H. D., and B. McKee, Stratigraphy of the Yakima Basalt in the type area, *Northwest Sci.*, *43*, 47–64, 1969.

DeGraff, J. M., P. E. Long, and A. Aydin, Use of joint-growth directions and rock textures to infer thermal regimes during solidification of basaltic lava flow, *J. Volcanol. Geotherm. Res.*, *38*, 309–324, 1989.

Dunlop, D. J., Determination of domain structure in igneous rocks by alternating field and other methods, *Earth Planet. Sci. Lett.*, *63*, 353–367, 1983.

Gillingham, D. E. W., and F. D. Stacey, Anhysteretic remanent magnetization (A. R. M.) in magnetite grains, *Pure Appl. Geophys.*, *91*, 160–165, 1971.

Graham, J. W., Changes of ferromagnetic minerals and their bearing on magnetic properties of rocks, *J. Geophys. Res.*, *58*, 243–260, 1953.

Grommé, C. S., T. L. Wright, and D. L. Peck, Magnetic properties and oxidation of iron-titanium oxide minerals in Alae and Makaopuhi lava lakes, Hawaii, *J. Geophys., Res.*, *74*, 5277–5293, 1969.

Haggerty, S. E., Opaque mineral oxides in terrestrial igneous rocks, in *Oxide Minerals*, edited by D. Rumble III, Chapter 8, pp. Hg101-Hg300, Mineralogical Society of America, Washington, D.C., 1976.

Herzog, M., H. Böhnel, H. Kohnen, and J. F. W. Negendank, Variation of magnetic properties and oxidation state of titanomagnetites within selected alkali-basalt flows of the Eifel-Area, Germany, *J. Geophys.*, *62*, 180–192, 1988.

Hill, R., and P. Roeder, The crystallization of spinel from basaltic liquid as a function of oxygen fugacity, *J. Geol.*, *82*, 709–729, 1974.

Johnson, H. P., W. Lowrie, and D. V. Kent, Stability of anhysteretic remanent magnetization in fine and coarse magnetite and maghemite particles, *Geophys. J. R. Astron. Soc.*, *41*, 1–10, 1975.

Kellerhals, R., J. Shaw, and V. K. Arona, On grain size from thin sections, *J. Geol.*, *83*, 79–96, 1975.

Levi, S., and R. T. Merrill, A comparison of ARM and TRM in magnetite, *Earth Planet. Sci. Lett.*, *32*, 171–184, 1976.

Lewis, R. T., A Faraday type magnetometer with an adjustable field independent gradient, *Rev. Sci. Instrum.*, *42*, 31–34, 1971.

Long, P. E., and B. J. Wood, Structures, textures, and cooling histories of Columbia River basalt flows, *Geol. Soc. Am. Bull.*, *97*, 1144–1155, 1986.

Long, P. E., M. G. Snow, and N. J. Davidson, Relationships between internal structures and petrographic textures of basalt flows: Example from a continental flood tholeiite province, *Publ. RHO-BWI-SA-67*, Rockwell Hanford Oper., Richland, Wash., 1980.

Lowrie, W., and M. Fuller, On the alternating field demagnetization characteristics of multidomain thermoremanent magnetization in magnetite, *J. Geophys. Res.*, *76*, 6339–6349, 1971.

Mackin, J. H., A stratigraphic section in the Yakima Basalt and Ellensburg Formation in south-central Washington, *Rep. Invest. Wash. Div. Mines Geol.*, *19*, 45 pp., 1961.

Myers, C. W., Yakima Basalt flows near Vantage, and from core holes in the Pasco Basin, Washington, Ph.D. thesis, 119 pp., Univ. of Calif., Santa Cruz, 1973.

Nag, S. K., Nature of primary oxidation and iron-titanium oxide mineralography in a single Rajmahal basalt lava, Bihar, *Indian J. Earth Sci.*, *12*, 135–140, 1985.

Nag, S. K., and S. B. Mallik, Temperature and oxygen fugacity of a lava flow from Rajmahal volcanics, Bihar, *Indian J. Earth Sci.*, *10*, 30–38, 1983.

O'Reilly, W., *Rock and Mineral Magnetism*, 220 pp., Blackie, Glasgow, 1984.

Osborn, E. F., Role of oxygen pressure in the crystalliation and differentiation of basaltic magma, *Am. J. Sci.*, *257*, 609–647, 1959.

Ozima, M., and M. Ozima, Characteristic thermomagnetic curve in submarine basalts, *J. Geophys. Res.*, *76*, 2051–2056, 1971.

Petersen, N., Notes on the variation of magnetization within basalt lava flows and dikes, *Pure Appl. Geophys.*, *114*, 177–193, 1976.

Reidel, S. P., and K. R. Fecht, Wanapum and Saddle Mountains Basalts of the Cold Creek Syncline area, Surface Geology of the Cold Creek Syncline, *Publ. RHO-BWI-ST-14*, chap. 3, pp. 1–45, Rockwell Hanford Oper., Richland, Wash., 1981.

Richards, J. C. W., J. B. O'Donovan, W. O'Reilly, and K. M. Creer, A magnetic study of titanomagnetite substituted by magnesium and aluminium, *Phys. Earth Planet. Inter.*, *7*, 437–444, 1973.

Sato, M., and T. L. Wright, Oxygen fugacities directly measured in magmatic gases, *Science*, *153*, 1103–1105, 1966.

Schönharting, G., Vermessung des Erdmagnetischen Feldes längs einiger Profile in Nord-Island, deren Auswertung und Interpretation, inauguraldissertation, Ludwig-Maximilians Univ. München, Munich, 1969.

Stacey, F. D., and S. K. Banerjee, *The Physical Principles of Rock Magnetism*, 195 pp., Elsevier, New York, 1974.

Stoner, E. C., and E. P. Wohlfarth, A mechanism of magnetic hysteresis in heterogeneous alloys, *Philos. Trans. R. Soc. London*, *A240*, 599–642, 1948.

Stormer, J. C., The effects of recalculation on estimates of temperature and oxygen fugacity from analyses of multicomponent iron-titanium oxides, *Am. Mineral.*, *68*, 586–594, 1983.

Swanson, D. A., T. L. Wright, and R. T. Helz, Linear vent systems and estimated rates of magma production and eruption for the Yakima Basalt on the Columbia Plateau, *Am. J. Sci.*, *275*, 877–905, 1975.

Verhoogen, J., Oxidation of iron-titanium oxides in igneous rocks, *J. Geol.*, *70*, 168–181, 1962.

Watkins, N. D., and S. E. Haggerty, Some magnetic properties and the possible petrogenetic significance of oxidized zones in an Icelandic olivine basalt, *Nature*, *206*, 797–800, 1965.

Watkins, N. D., and S. E. Haggerty, Primary oxidation variation and petrogenesis in a single lava, *Contrib. Mineral. Petrol.*, *15*, 251–271, 1967.

Wilson, R. L., N. D. Watkins, and S. E. Haggerty, Variation of paleomagnetic stability and other parameters in a vertical traverse of a single Icelandic lava, Geophys. *J. R. Astron. Soc.*, *16*, 79–96, 1968.

Wones, D. R., and M. C. Gilbert, The fayalite-magnetite-quartz assemblage between 600° and 800°C, *Am. J. Sci.*, *267-A*, 480–488, 1969.

H. Audunsson, Hvassaleiti 157, 103 Reykjavik, Iceland.

F. Hodges, Westinghouse, Hanford Operations, PO Box 1970, Richland, WA 99352.

S. Levi, College of Oceanography, Oregon State University, Ocean Admin Bldg 104, Corvallis, OR 97331-5503.

(Received May 31, 1990;
revised April 17, 1991;
accepted June 5, 1991.)